ECOHYDROLOGY
Ecohydrol. **9**, 248–266 (2016)
Published online 24 April 2015 in Wiley Online Library
(wileyonlinelibrary.com) DOI: 10.1002/eco.1629

Monthly land cover-specific evapotranspiration models derived from global eddy flux measurements and remote sensing data

Yuan Fang,[1] Ge Sun,[2]* Peter Caldwell,[3] Steven G. McNulty,[2] Asko Noormets,[1] Jean-Christophe Domec,[1,4] John King,[1] Zhiqiang Zhang,[5] Xudong Zhang,[6] Guanghui Lin,[7] Guangsheng Zhou,[8] Jingfeng Xiao[9] and Jiquan Chen[10]

[1] *Department of Forestry and Environmental Resources, North Carolina State University, Raleigh, NC, USA*
[2] *Eastern Forest Environmental Threat Assessment Center, Southern Research Station, USDA Forest Service, Raleigh, NC, USA*
[3] *Coweeta Hydrologic Laboratory, Southern Research Station, USDA Forest Service, Otto, NC, USA*
[4] *University of Bordeaux, Bordeaux Sciences Agro UMR INRA-ISPA 1391, Gradignan, France*
[5] *College of Soil and Water Conservation, Beijing Forestry University, Beijing, China*
[6] *Institute of Forest Research, Chinese Academy of Forestry, Beijing, China*
[7] *Center for Earth System Science, Tsinghua University, Beijing, China*
[8] *Institute of Botany, Chinese Academy of Sciences, Beijing, China*
[9] *Earth Systems Research Center, University of New Hampshire, Durham, NH, USA*
[10] *Center for Global Change and Earth Observations (CGCEO), and Department of Geography, Michigan State University, East Lansing, MI, USA*

ABSTRACT

Evapotranspiration (ET) is arguably the most uncertain ecohydrologic variable for quantifying watershed water budgets. Although numerous ET and hydrological models exist, accurately predicting the effects of global change on water use and availability remains challenging because of model deficiency and/or a lack of input parameters. The objective of this study was to create a new set of monthly ET models that can better quantify landscape-level ET with readily available meteorological and biophysical information. We integrated eddy covariance flux measurements from over 200 sites, multiple year remote sensing products from the Moderate Resolution Imaging Spectroradiometer (MODIS), and statistical modelling. Through examining the key biophysical controls on ET by land cover type (i.e. shrubland, cropland, deciduous forest, evergreen forest, mixed forest, grassland, and savannas), we created unique ET regression models for each land cover type using different combinations of biophysical independent factors. Leaf area index and net radiation explained most of the variability of observed ET for shrubland, cropland, grassland, savannas, and evergreen forest ecosystems. In contrast, potential ET (PET) as estimated by the temperature-based Hamon method was most useful for estimating monthly ET for deciduous and mixed forests. The more data-demanding PET method, FAO reference ET model, had similar power as the simpler Hamon PET method for estimating actual ET. We developed three sets of monthly ET models by land cover type for different practical applications with different data availability. Our models may be used to improve water balance estimates for large basins or regions with mixed land cover types. Copyright © 2015 John Wiley & Sons, Ltd.

KEY WORDS eddy covariance flux; evapotranspiration; ecosystem modelling; ecohydrology; FLUXNET

Received 12 August 2014; Revised 25 January 2015; Accepted 16 March 2015

INTRODUCTION

Global climate and land use changes directly affect the hydrological cycle (Caldwell *et al*., 2012), water resources (Sun *et al*., 2008; Thompson *et al*., 2014), and ecosystem services (King *et al*., 2013) by altering evapotranspiration (ET) processes at multiple scales. ET is tightly coupled with the ecosystem energy balance (Chen *et al*., 2004; Sun *et al*., 2010) and carbon balance (Law *et al*., 2002; Beer *et al*., 2007; Beer *et al*., 2010; Sun *et al*., 2011a; Tian *et al*., 2011), and thus plays an important role in the climatic feedback between land surface and climate systems (Baldocchi *et al*., 2001; Bonan, 2008; Cheng *et al*., 2011). In spite of the importance of quantifying ET for various ecosystems (Baldocchi and Ryu, 2011; Shuttleworth, 2012), accurate quantification of watershed to regional scale ET remains costly and uncertain due to the highly dynamic nature of ET processes (Sun *et al*., 2011a; Li *et al*., 2012; McMahon *et al*., 2012; Jasechko *et al*., 2013).

There are many ways to quantify ET at different temporal and spatial scales (Jackson *et al*., 2000; Shuttleworth, 2012). Direct ecosystem-scale ET measure-

*Correspondence to: Ge Sun, Eastern Forest Environmental Threat Assessment Center, Southern Research Station, USDA Forest Service, Raleigh, NC 27606, USA.
E-mail: gesun@fs.fed.us

ment techniques include catchment water balance (Bosch and Hewlett, 1982), sap flow (Smith and Allen, 1996), eddy covariance (Baldocchi *et al*., 2001), and Bowen Ratio methods. Remote sensing techniques allow monitoring ET at a very large spatial scale (Kustas and Norman, 1996). Wilson *et al*. (2001), and more recently, Domec *et al*. (2012a) compared multiple direct ET measurement methods and found that each method had its own limitations. The eddy covariance method measures site-level fluxes continuously, offering high temporal resolution data series and representing perhaps the most accurate method in ecohydrological studies during the past two decades. Remote sensing has been widely used to estimate global ET (Justice *et al*., 1998; Ray and Dadhwal, 2001; Mu *et al*., 2007, 2010; Mu *et al*., 2011; Song *et al*., 2011), and the accuracy of the resulting gridded products is often assessed using eddy covariance flux measurements.

Because of the high cost of measuring ET directly (e.g. eddy flux methods) or estimating at large scales (i.e. watershed to regional), mathematical modelling has been widely used to estimate ET (see review in McMahon *et al*., 2012). The empirical ET models developed by Zhang *et al*. (2001), Sun *et al*. (2011a, b), and Zeng *et al*. (2012) capture the basic biophysical controls on ET including leaf area index (LAI), water, and energy availability (Feng *et al*., 2012; Hoy, 2012). However, these models clearly have deficiencies. For example, while these models take into account differences in LAI among land cover types, the same equation is used for all land cover types that does not differentiate the influence of biome-specific physiological characteristics (e.g. canopy conductance, rooting depth, and water use efficiency) on ET processes (Mackay *et al*., 2007). The literature shows that ET rates vary across different vegetation cover types under similar climatic and meteorological conditions (Dunn and Mackay, 1995; Liu *et al*., 2010).

The objectives of this study were to (1) examine the environmental controls of ET in terrestrial ecosystems at a monthly time scale by combining ET measurements from the global eddy covariance flux network and remote sensing data, and (2) create a new set of ET models to improve the previous ET models (Sun *et al*., 2011a, 2011b) by separating land cover types. We used the following hypotheses to guide our analysis: (1) the variables most important in explaining observed monthly ET variability differ among land cover types, (2) separating land cover type improves model accuracy from lumped models, and (3) monthly ET can be modelled sufficiently using simple energy and water availability variables, such as potential ET (PET) and precipitation, and LAI.

DATA AND METHODS

Several large time series databases were used to develop the ET models. Mean values of daily ET and other environmental variables were used to derive monthly values from mean daily values. We first corrected the reported daily ET by closing the energy balance. Then, we combined the corrected monthly ET, monthly total P, mean MODIS LAI, other monthly environmental variables (e.g. mean VPD), and PET data into one dataset. We associated all these variables with land cover types. The database spanned seven years (2000–2006) and included 9637 site-month records.

FLUXNET La Thuile ET database

This study combined site-level remote sensing data and La Thuile eddy flux database developed by the FLUXNET (http://www.eosdis.ornl.gov/FLUXNET) – a global network that measures the exchanges of carbon dioxide, water vapour, and energy between the biosphere and atmosphere (Baldocchi *et al*., 2001; Figure 1). FLUXNET data have been widely used to quantify the dynamics of regional and global ecosystem carbon and water balances (Beer *et al*., 2010; Jung *et al*., 2010; Williams *et al*., 2012; Xiao *et al*., 2012), and to validate various ecosystem models in which ET is a major control to the biogeochemical processes (Tian *et al*., 2011; Tian *et al*., 2012). The La Thuile ET database derived from a synthesis effort by FLUXNET consisted of 218 sites for the time period of 2000–2006 (Figure 1). These flux sites spanned a wide range of climate and physiographic regions in both hemispheres and on five continents with latitudinal distribution that ranged from 70° north to 30° south. The mean annual precipitations ranged from 93 (RU-Che, North Russia, snow dominated) to 2633 mm (CN-Anh, East China), and the mean annual temperature ranged from −5.8 (RU-Che) to 26.6 C (ID-Pag, North Indonesia) (Figure 2). The database included 4 sites in savannas (SAV), 5 sites in closed shrubland (CS), 10 sites in open shrubland (OS), 12 sites in mixed forest (MF), 17 sites in evergreen broad leaf forest (EBF), 29 sites in deciduous broad leaf forest (DB), 31 sites in cropland (CRO), 44 sites in grassland (GRA), and 66 sites in evergreen needleleaf forest (ENF).

In addition to the ET measurements, the La Thuile database included biophysical variables that were used to explain the variability in ET. The variables used study included daily latent heat flux (LE, $MJ\,m^{-2}$), air temperature (Ta, °C), vapour pressure deficit (VPD, 100 Pa), precipitation (P, mm), net radiation (Rn, $MJ\,m^{-2}$), sensible heat flux (H, $MJ\,m^{-2}$), and soil heat flux (G, $MJ\,m^{-2}$). General site characteristics including the International Geosphere-Biosphere Program (IGBP) vegetation classification, latitude, and longitude were also collected. The daily flux data were scaled from half-hour eddy covariance measurements (Valentini *et al*., 2000; Baldocchi *et al*., 2001).

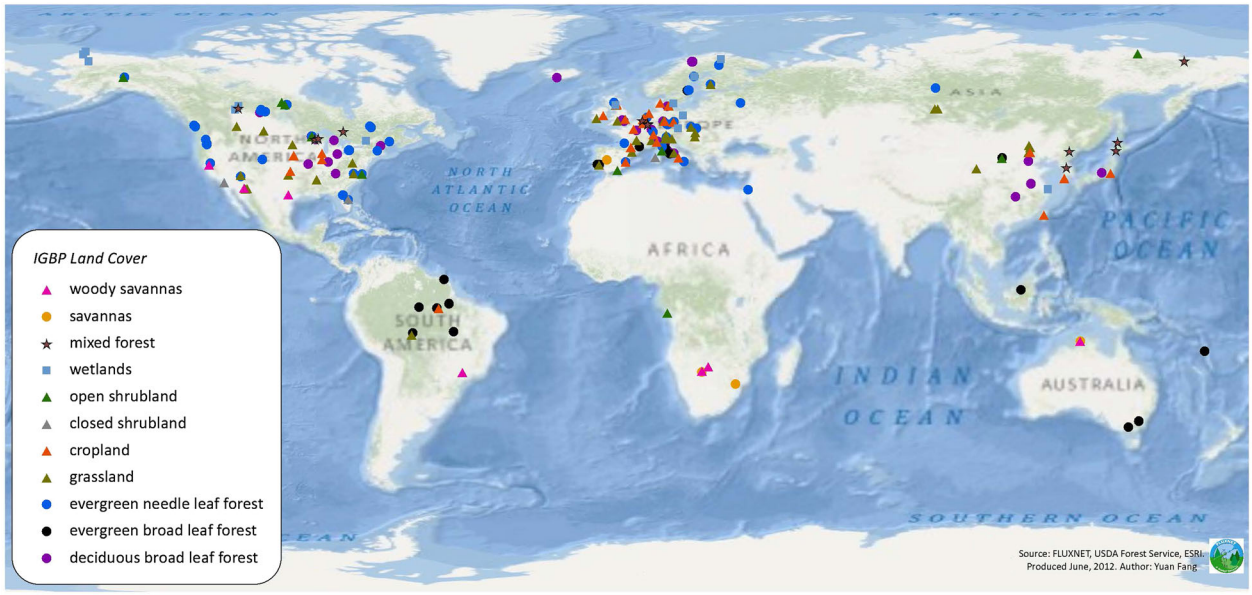

Figure 1. Distribution of FLUXNET research site and IGBP land cover type.

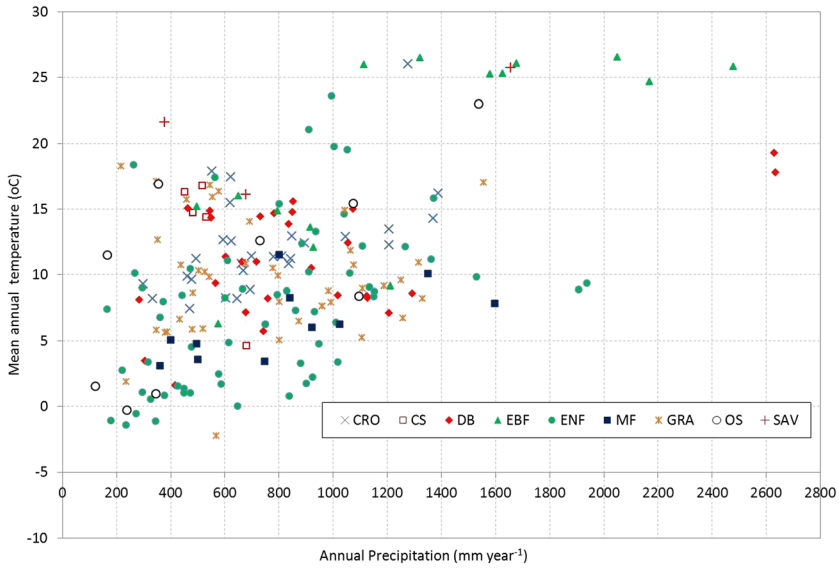

Figure 2. Distribution of annual mean temperature and precipitation. CRO, cropland; CS, closed shrubland; DB, deciduous broadleaf forest; EBF, evergreen broadleaf forest; ENF, evergreen needleleaf forest; GRA, grassland; MF, mixed forest; OS, open shrubland; SAV, savannas.

Uncertainties exist in the La Thuile data including measurement errors and misunderstanding of computing methods (Hollinger and Richardson, 2005). Data were considered erroneous or outliers and were removed from the database records when daily Rn exceeded 100 MJ m^{-2}, daily LE or H exceeded 25 MJ m^{-2}, calculated daily PET was negative, ET exceeded 300 mm $month^{-1}$, or VPD was negative. In addition, when estimating monthly sums from monthly mean using daily data, we removed those months with the number of day less than 15 days and the data gaps were centered within the month time span. As result, the number of sites used varied in this study for developing different models and analyses at different temporal scales.

We used an integrated procedure (Figure 3) to process the La Thuile database of eddy flux measurements from 218 sites. According to the IGBP land cover classification system, these eddy flux sites cover nine land cover types: shrubland including both closed (CS) and open shrubland (OS), cropland (CRO), grassland (GRA), deciduous broad leaf forest (DB), evergreen needleleaf forest (ENF) and evergreen broad leaf forest (EBF), mixed forest (MF), and savannas (SAV). For each eddy flux tower site (Figure 1),

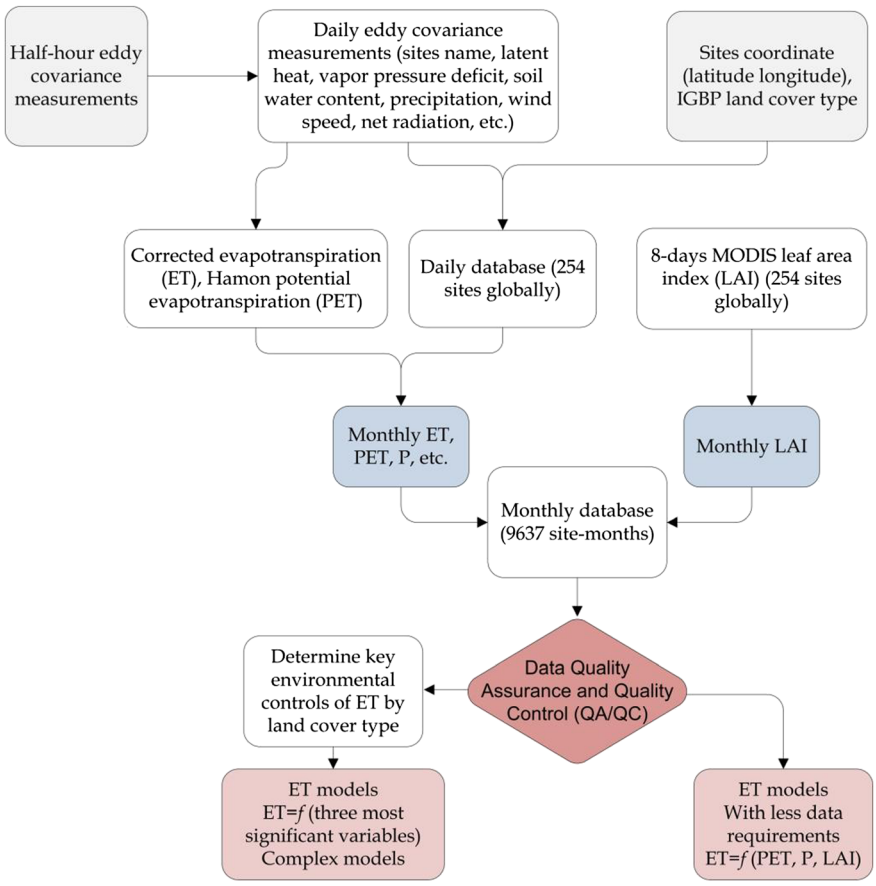

Figure 3. An overview of research methods for database development and analysis.

we acquired ET and associated micro-meteorological data, and built relational databases of ET, VPD, P, wind speed, and Rn. PET was calculated from mean monthly air temperature using the Hamon's method (see detailed description later).

Leaf area index data from MODIS products

Leaf area index represents projected leaf surface area per unit ground area ($m^2\,m^{-2}$). The development of remote sensing techniques made global LAI measurements available at a large range of spatial resolutions and short time interval (Asrar *et al*., 1983; Running, 1984; Running *et al*., 1989). LAI has been widely used in understanding ecosystem processes and building ET and hydrological models (Cramer *et al*., 1999; Sun *et al*., 2011a, 2011b).

The LAI time series for each tower site was downloaded from the Oak Ridge National Laboratory Distributed Active Archive Center (http://daac.ornl.gov/cgi-bin/MODIS/GR_col5_1/mod_viz.html). MODIS LAI was derived from the fraction of absorbed photosynthetically active radiation (FPAR) that a plant canopy absorbs for photosynthesis and growth in the 0.4–0.7 nm spectral range. LAI is the biomass equivalent of FPAR. The MODIS LAI/FPAR algorithm exploits the spectral information of MODIS surface reflectance at up to seven spectral bands. We extracted monthly LAI data for the time period from 2000 through 2006 across 254 sites using 8-day GeoTIFF data from the Moderate Resolution Imaging Spectroradiometer (MODIS) land subsets' 1-km LAI global fields. First, we downloaded 8-day data for each site based on latitude and longitude. We then converted image data into a grid format and multiplied by a scale factor (0.1) to get the true value of LAI (Mu *et al*., 2011). We estimated monthly LAI by computing the mean of the 8-day daily values for each month, and finally, we extracted individual time series data from the grid cells containing each tower site.

Evapotranspiration correction

The latent heat (LE) flux represents energy absorbed for water to change from the liquid state to vapour phase without a change in temperature through the ET process. The ET rates were calculated from LE with a conversion factor, constant of heat vaporization. According to literature (Wilson *et al*., 2002; Foken, 2008), the LE can be underestimated by as much as 20% because of a lack of energy balance closure. Previous studies suggest that the incomplete energy closure issues were mainly caused by

inaccurate estimation of available energy, incomplete energy balances (e.g. heat storage term is often neglected) (Mayocchi and Bristow, 1995), a changing source area of turbulent fluxes (Schmid, 1997; Shao *et al*., 2014), and large mobility of the turbulent flux and flux sampling errors (Mahrt, 1998).

We corrected the daily ET estimates using the method by Twine *et al*. (2000) to account for the energy conservation discrepancy in eddy flux measurements. This method redistributed the residual of available energy (Rn minus G) and the sum of latent heat and sensible heat ($H+\mathrm{LE}$) back to both LE and H by maintaining the Bowen Ratio (H/LE) such that

$$\mathrm{ET_c} = \mathrm{ET} \times \frac{\mathrm{Rn} - G}{H + \mathrm{LE}}$$

where $\mathrm{ET_c}$ is the corrected daily ET (mm), Rn is the net radiation (MJ $\mathrm{m^{-2}}$), G is the daily soil heat flux (MJ $\mathrm{m^{-2}}$), H is the sensible heat flux (MJ $\mathrm{m^{-2}}$), and LE is the latent heat flux (MJ $\mathrm{m^{-2}}$).

Potential evapotranspiration estimation

Potential evapotranspiration is widely used in modelling actual ET and streamflow, and it sets an upper limit of actual ecosystem water loss assuming unlimited soil water availability (Lu *et al*., 2003; Lu *et al*., 2005; Sun *et al*., 2011a). Hamon's (1963) PET method was used in this study because of its simplicity and wide use (Vörösmarty *et al*., 1998; Lu *et al*., 2005). The Hamon PET method computes daily ET based on air temperature and daytime length

$$\mathrm{PET} = 0.1651 \times \mathrm{DAY} \times \frac{216.7 \times e_\mathrm{s}}{t_\mathrm{a} + 273.3}$$

where PET is the daily potential ET (mm), DAY is the day length in multiples of 12 h calculated as a function of latitude (Lat) and Julian day, e_s is the saturation vapour pressure at a given temperature, and t_a is the mean air temperature (°C).

The saturation vapour pressure, e_s, is computed as follows:

$$e_\mathrm{s} = 6.108 \times e \frac{17.2694 \times t_\mathrm{a}}{t_\mathrm{a} + 237.3}$$

The day length is computed as follows:

$$\mathrm{DAY} = 2 \times \mathrm{acos}\left(-1 \times \tan(\mathrm{Lat} \times 0.0175) \times \tan\left(0.4093 \times \sin\left(\frac{2*3.1415*\mathrm{DoY}}{365.0}\right) - 1.405\right)\right)/3.14159$$

where DoY is the Julian day of the year ranging between 1 and 366.

The FAO grass reference ET ($\mathrm{ET_o}$) method has been widely used to characterize local meteorological conditions or PET in reference to a standard land cover, such as a short grass (Allen *et al*., 1994). Daily $\mathrm{ET_o}$ is calculated by the process-based Penman–Monteith ET equation parameterized for a hypothetical well-watered grass that has a 0.12 m canopy height, a leaf area of 2.8, a bulk surface resistance of 70 s $\mathrm{m^{-1}}$, and an albedo of 0.23 as estimated as follows:

$$\mathrm{ET_o} = \frac{0.408\Delta(\mathrm{Rn} - G) + \gamma \frac{C}{T+273} u_2 (e_\mathrm{s} - e_\mathrm{a})}{\Delta + \gamma(1 + 0.34\mu_2)},$$

where $\mathrm{ET_o}$ is the grass reference ET (mm $\mathrm{day^{-1}}$), Δ is the slope of the saturation water vapour pressure at air temperature T (kPa °$\mathrm{C^{-1}}$),

$$\Delta = 2503 \frac{e^{\frac{17.27T}{T+237.3}}}{(T + 237.3)^2},$$

Rn is the net radiation (MJ $\mathrm{m^{-2}}$), G is the soil heat flux (MJ $\mathrm{m^{-2}}$), γ is the psychrometric constant (kPa °$\mathrm{C^{-1}}$), e_s is the saturation vapour pressure (kPa), e_a is the actual vapour pressure (kPa), u_2 is the mean wind speed (m $\mathrm{s^{-1}}$) at 2 m height, and C is the unit conversion factor with a value of 900.

Development of monthly ET model using regression analysis

The global flux sites represent contrasting biomes under a wide range of climatic regimes and management conditions (i.e. irrigated croplands and plantation forests). After conducting data quality assessment and quality control, we selected the best independent variables for predicting ET using Pearson correlation metrics. We examined different combinations of biophysical variables to achieve the best model fit for each of the eight ecosystem types. The multivariate linear regression procedures in the SAS 9.2 software (SAS Institute Inc., 2008) were used for model development. Combinations of key biophysical factors were examined to achieve the best model fit. For each regression model, collinearity issues among independent variable were assessed by computing the variance inflation factor (VIF; Marquard, 1970). A VIF above 5 indicated collinearity among independent variables, and the variables would be removed from the linear regression models.

We created three sets of empirical ET models to meet the requirements of different types of potential users and test whether a model with higher complexity improves predictability. Type I models were developed using the most significant variables (Rn, P, LAI, and PET) that potentially maximized model accuracy. Type II models

were constructed using only three biophysical variables (P, PET, and LAI) that are readily available from standard weather monitoring stations and regional remote sensing products (LAI) (Sun *et al.*, 2011a, b). Type III models were similar to Type II except that PET variable was replaced with ET_o, calculated by the more robust but also more data-demanding FAO reference ET equation. We evaluated the model performance at two different levels: overall model performance by biome type across all sites, and site-specific model performance at two forest sites. To assess model performance by biome type, we compared our models separating land cover types with models by lumping all land cover types (Sun *et al.*, 2011a, b). To assess site-specific model performance, we applied the generalized ET model developed for evergreen needleleaf forest (ENF) to two flux sites with contrasting climatic characteristics and examined potential modelling errors. We used coefficients of determination (R^2) and root of mean square error (RMSE) to quantitatively evaluate model performance.

RESULTS

Long-term mean annual ET rates for any ecosystems are primarily controlled by water (P) and energy (PET) availability. This section presents both mean annual and seasonal relationships among ET, PET, and P using the Budyko (1974) framework. We used the Hamon PET for this analysis after we have found that this method was more dependable for more ecosystems than the ET_o had. Although PET and ET_o were highly correlated on average across all sites, the ET_o method gave about 30% higher estimates of ET than the Hamon PET model (not shown). Across all sites, the mean annual ET was 474 mm, while the mean annual PET and ET_o was 1030 and 750 mm, respectively.

The ET, PET, ET_o, and P relationship at annual scale

Annual P and PET rates varied dramatically among the biomes. The majority of evergreen broadleaf forest (EBF) was found in a tropical climate with a mean annual P of 1330 mm and mean PET of 1087 mm. In contrast, evergreen needleleaf forest (ENF) had a much wider range, with PET ranging from 450 to 1300 mm (mean = 635 mm) and P from 166 to 1907 mm (mean = 785 mm). Deciduous forest (DB) had the highest range in P (250–2500 mm), with a mean of 908 mm and PET from 500 to 1144 mm (mean PET = 702 mm). Fewer flux sites were found in mixed forest (MF); the 12 sites examined by this study had a very narrow range in PET (521–684 mm) with a mean of 572 mm, but a large P ranging from 93 to 1600 mm (mean = 727 mm). Grassland sites had a wide range of P (~236–1316 mm) with a mean of 750 mm, and a large range of PET (mean = 687 mm) varying from 313 to 1032 mm. There was substantial overlap in the ranges of P and PET between grassland and DB. The 31 cropland (CRO) sites were found in a warmer climate than grasslands and also had a wide range of PET (551–1453 mm, mean = 788) and P (333–1389 mm, mean = 774 mm). Similar to grasslands, the shrublands had a large range in P, varying from 123 to 1500 mm. The ranges of P and PET for shrublands (CS and OS) (mean P = 594 mm, PET = 781 mm) and savannas (SAV) sites (mean P = 673 mm, PET = 1134 mm) overlapped with those for grasslands. Annual PET rates exceeded 400 mm for all ecosystems but one (CN-Ham, Haibei Alpine Tibet site in

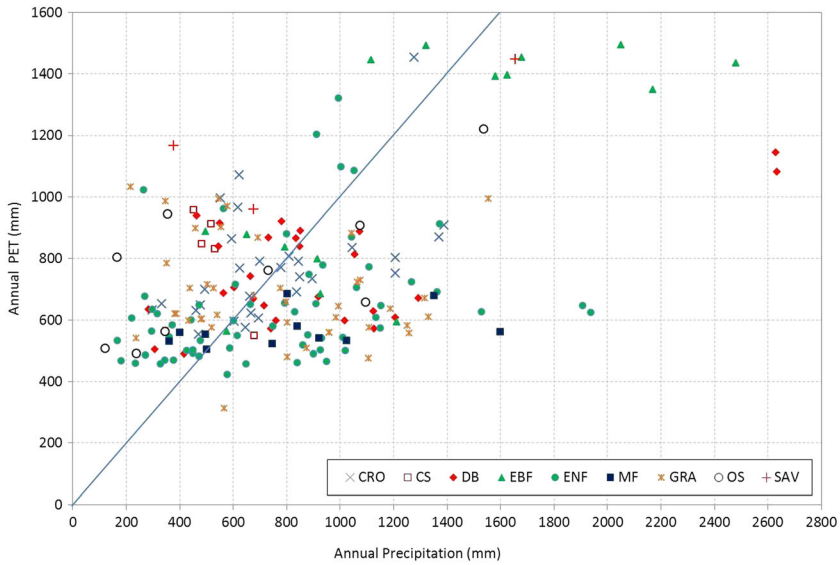

Figure 4. Distribution of mean annual PET and precipitation. CRO, cropland; CS, closed shrubland; DB, deciduous broad leaf forest; EBF, evergreen broad leaf forest; ENF, evergreen needleleaf forest; GRA, grassland; MF, mixed forest; OS, open shrubland; SAV, savannas.

China) where PET was only 313 mm and mean air temp was −2.2 °C (Figure 4).

Annual total ET exceeded P at 35 out of the 137 sites (Figure 5a and b). Notably, the ET of the three cropland sites (ES-ES2 in Spain, IT-Cas in Italy, and US-IB1 in the US) (889–1048 mm) was much higher than P (553–623 mm) (Group 1, Figure 5). The three sites received substantial irrigation (Cheng *et al.*, 2011), leading to much higher ET compared with P. Among the other three forest sites in Group 1 (Figure 5), Wisconsin US-Wi1 and US-Wi2 located in the lowlands had an ET of 776 and 673 mm, respectively. The P for the US-Wi1 and US-Wi2 was only 284 and 297 mm, respectively. These two sites likely received supplemental groundwater to meet the ET demand. The other forest site (CN-Bed, Beijing, China) in Group 1 was a highly productive poplar plantation that received irrigation in the spring when drought occurred (Zhou *et al.*, 2013).

We also found that ET exceeded Hamon PET at 22 out of the 137 sites, particularly US-Wi1, two grassland sites in Italy (IT-MBo and IT-Mal), an evergreen needleleaf forest (ENF) site in Nebraska (US-NR1), a pine plantation in North Carolina on coastal wetlands (NC2) (Sun *et al.*, 2010), and an alpine grassland in China (CN-HaM).

The ET, PET, ET_o, and P relationship at the growing season scale

The ET fluxes for vegetated surfaces were the highest during the growing season. Total ET in the growing season

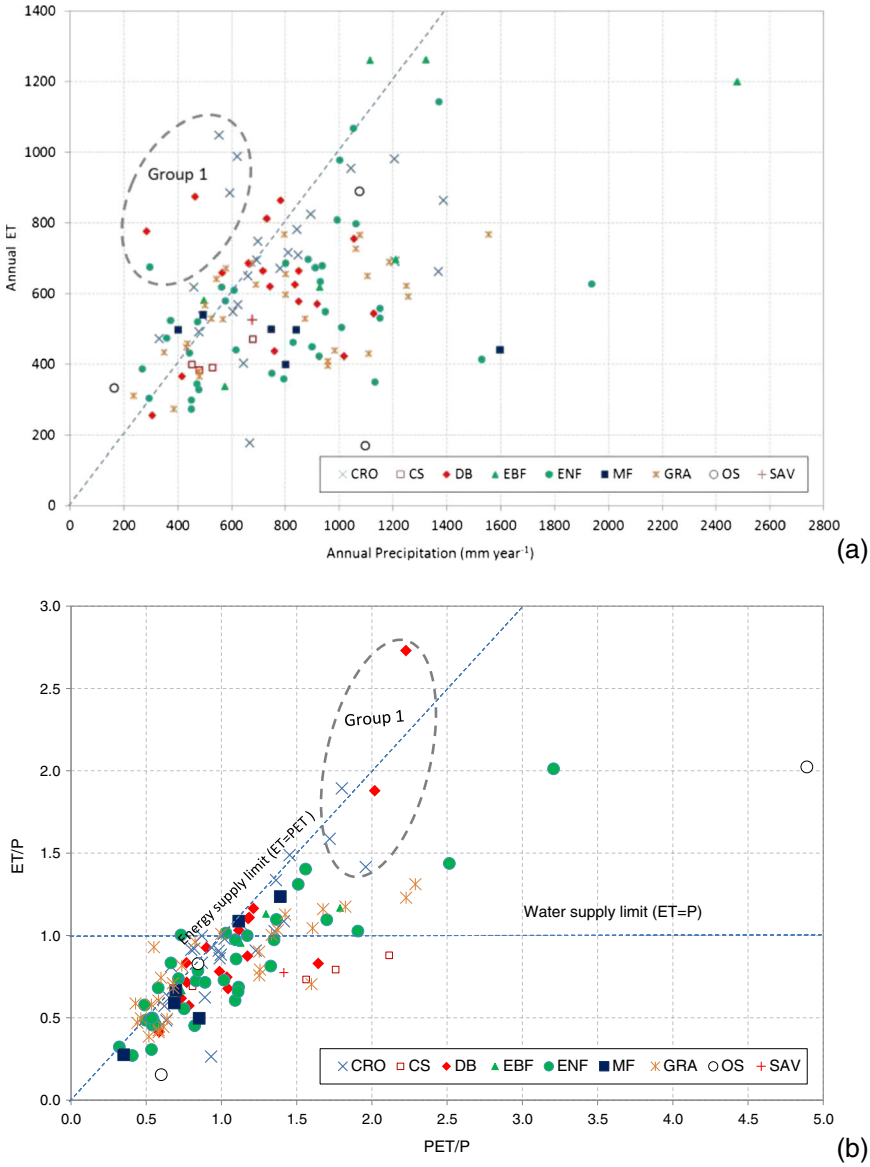

Figure 5. A comparison of (a) mean annual ET versus precipitation (P), and (b) mean Evaporative Index (ET/P) and Dryness Index (PET/P) in the Budyko (1974) framework, for all FLUXNET sites used in the analysis. CRO, cropland; CS, closed shrubland; DB, deciduous broad leaf forest; EBF, evergreen broad leaf forest; ENF, evergreen needleleaf forest; GRA, grassland; MF, mixed forest; OS, open shrubland; SAV, savannas.

exceeded P at about 60% of the study sites (Figure 6). When growing season ET exceeded P, ecosystem water use was supplied not only by growing season P but also by soil water storage, the 'old water'. Evergreen needleleaf forest (ENF) and grassland (GRA) sites spread almost equally around the 1:1 line, suggesting that there sites have a wide range of growing season climatic regimes. Mixed forest (MF), closed shrubland (CS), and cropland (CRO) sites were mostly found with ET exceeding P. A few CRO sites had much higher ET than P in the growing season, presumably due to irrigation. As expected, growing season P exceeded ET greatly for evergreen broad leaf forest (EBF) in a wet tropical environment. Most interestingly, ET was close to or greater than P at all deciduous broad leaf forest (DB) sites except one, suggesting that soil water storage was more important for supplying ET demand in DB ecosystems than in other ecosystems over the growing seasons.

Key environmental controls on ET

Energy availability (PET or Ta, Rn), atmospheric dryness (VPD), and plant biomass (LAI) were the top five influential variables for predicting ET at the monthly scale across all sites (Table I). Interestingly, water availability as represented by total precipitation (P) did not correlate well with ET. As expected, overall, the energy terms (Rn, PET, and Ta) were highly correlated among themselves, moderately correlated with LAI but weakly with VPD (Table I).

When examining the data by ecosystem type, there were similarities and differences among the key variables for explaining the variability of measured ET (Table II). Rn and LAI correlated consistently well with ET for all ecosystems. Precipitation (P) was not as influential as other five variables (Pearson correlation coefficients < 0.32) for all biomes. For shrublands, energy and air humidity indicators (Ta, PET, and Rn) and VPD, respectively, did not correlate with ET. Instead, LAI could explain 77% of the variability of ET.

Table I. Pearson correlations betweeb evapotranspiration (ET) and indpendent variables for all biomes represenetd by the the entire FLUXNET dataset.

	ET	Ta	VPD	PET	P	Rn	LAI
ET	1.00	0.66	0.34	0.71	.	0.75	0.50
Ta	0.66	1.00	0.74	0.93	.	0.73	0.42
VPD	0.34	0.74	1.00	0.78	.	0.61	.
PET	0.71	0.92	0.78	1.00	.	0.81	0.41
P	.	.	.	.	1.00	.	.
Rn	0.75	0.73	0.61	0.81	.	1.00	0.43
LAI	0.50	0.42	.	0.41	.	0.43	1.00

Only correlation coefficients greater than 0.3 or less than −0.3 are shown. Ta, air temperature; VPD, vapour pressure deficit; PET, potential evapotranspiration; P, precipitation; Rn, net radiation; LAI, leaf area index.

Stepwise regression analysis by ecosystem type revealed complex relationships between ET and environmental controls (Table III). The environmental factors could be represented by a different set of key independent variables for different ecosystems. For example, PET alone explained 79% ($p < 0.0001$) of the variability of ET for mixed forest (MF). In contrast, LAI and VPD (total partial $R^2 = 0.69$) were most useful for estimating ET of Savannas ecosystem.

Monthly ET models. The Type I regression models for each land cover type (Table IV) consist of the top three

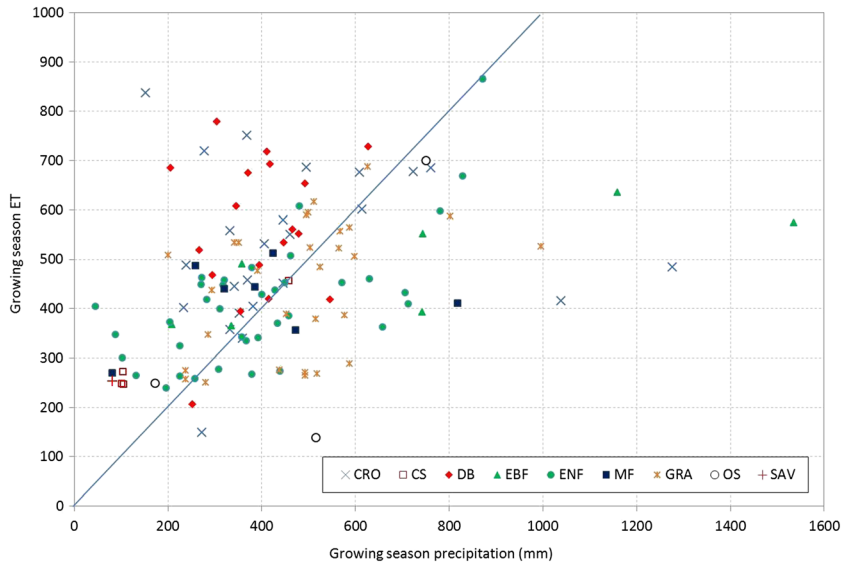

Figure 6. Distribution of growing season mean ET and precipitation. CRO, cropland; CS, closed shrubland; DB, deciduous broad leaf forest; EBF, evergreen broad leaf forest; ENF, evergreen needleleaf forest; GRA, grassland; MF, mixed forest; OS, open shrubland; SAV, savannas.

Table II. Pearson correlation coefficient (PCC) between monthly evapotranspiration and biophysical parameters for different land cover types.

Land cover type	Ta	PET	LAI	Rn	VPD	P
Shrubland	0.54	0.6	0.77	0.5	.	.
Cropland	0.74	0.82	0.59	0.81	0.60	.
Grassland	0.71	0.79	0.50	0.86	0.51	.
Deciduous broadleaf forest	0.77	0.85	0.66	0.82	0.62	.
Evergreen needle leaf forest	0.78	0.80	0.57	0.79	0.65	.
Evergreen broad leaf forest	0.86	0.87	0.29	0.87	0.62	.
Mixed forest	0.79	0.89	0.71	0.86	0.79	.
Savannas	.	.	0.71	0.49	.	.

Only correlation coefficients greater than 0.3 or less than −0.3 are shown. Ta, air temperature; VPD, vapour pressure deficit; PET, potential evapotranspiration; P, precipitation; Rn, net radiation; LAI, leaf area index.

most significant independent variables ($p < 0.03$) as identified in Table III. The three variables in each of models did not have co-linearity as determined by VIF values (<5.0). The models had R^2 varying from 0.66 to 0.86, and RMSE ranging from 14.2 to 23.9 mm month^{-1}.

Similar to the Type I models, the R^2 values for Type II models varied from 0.66 to 0.80 (Table V). However, the Type II models had much lower R^2 values for both GR and BF biomes. The mean RMSE for the Type I models (mean = 17.0 with a range of 13.3–23.9 mm month^{-1}) was almost identical to that for the Type II models (mean = 16.6 with a range of 11.1–23.7 mm month^{-1}). For the Type II models, the selected variables (PET, LAI, and P) were highly significant ($p < 0.0001$) except for P for DB, EBF, and MF. PET was the only significant independent variable for predicting ET for MF.

Compared with the Type I and Type II models, the Type III models had slightly lower R^2, varying from 0.49 for EBF to 0.77 for MF. However, the R^2 for SVA (0.74) in the Type III model was much higher than those in Type I (0.66) and Type II (0.68) models. The RMSE for the Type III models was 17.0 (11.8–23.3 mm month^{-1}), almost identical to the Type II model. In contrast to the Type I and Type II models, all three variables (ET_o, LAI, and P) in the Type III models were highly significant ($p < 0.001$) for all biomes except for EBF where LAI was not a significant factor.

Table III. The most significant variables contributed to evapotranspiration with their partial R^2 values of different land cover types.

Land cover type	Partial R^2 of significant variables						
	Ta	PET	LAI	Rn	P	VPD	*n*
Shrubland	.	0.04	0.60	0.19	.	.	123
Cropland	.	0.67	0.01	0.04	.	0.03	609
Grassland	.	0.04	0.04	0.75	.	0.01	802
Deciduous broadleaf forest	.	0.73	.	0.04	.	0.06	636
Evergreen needle leaf forest	.	0.64	0.04	0.05	0.02	.	1360
Evergreen broad leaf forest	0.01	0.76	.	0.11	.	.	190
Mixed forest	.	0.79	.	0.04	.	.	261
Savannas	.	0.05	0.50	0.16	.	0.19	36

All R^2 have *p* values less than 0.0001; only top four significant variables listed. Ta, air temperature; VPD, vapour pressure deficit; PET, potential evapotranspiration; P, precipitation; Rn, net radiation; LAI, leaf area index.

Table IV. Type I models by land cover type developed using the three most significant variables.

Land cover type	Model by land cover (Type I)	Model by land cover		Lump model		*n*
		RMSE	R^2	RMSE	R^2	
Shrubland	ET = 0.51 + 0.03 * PET + 14.73 * LAI + 0.08 * Rn	14.0	0.79	25.9	0.39	220
Cropland	ET = 0.87 + 0.19 * Rn + 13.99 * LAI + 0.06 * P	23.9	0.73	17.3	0.73	655
Grassland	ET = 5.55 + 7.23 * LAI + 0.20 * Rn	16.3	0.79	15.8	0.73	835
Deciduous forest	ET = −14.22 + 0.74 * PET + 0.10 * Rn	22.2	0.77	15.9	0.77	788
Evergreen needle leaf forest	ET = 3.00 + 0.30 * PET + 3.99 * LAI + 0.09 * Rn	17.1	0.71	18.2	0.69	1507
Evergreen broad leaf forest	ET = −0.15 + 0.47 * PET + 0.13 * Rn	13.3	0.86	11.6	0.85	246
Mixed forest	ET = −8.76 + 0.95 * PET	14.8	0.80	12.1	0.84	274
Savannas	ET = −8.07 + 33.46 * LAI + 0.07 * Rn	14.0	0.66	35.15	0.04	36

RMSE, root of mean square error; ET, evapotranspiration; PET, potential evapotranspiration; P, precipitation; Rn, net radiation; LAI, leaf area index.

Table V. Type II models by land cover type developed using three commonly measured biophysical variables.

Land cover type	Model by land cover (Type II)	Model by land cover type		Lumped model		
		RMSE	R^2	RMSE	R^2	n
Shrubland	ET = −3.11 + 0.39 * PET + 0.09 * P + 11.127 * LAI	12.5	0.80	18.8	0.64	193
Cropland (CRO)	ET = −8.15 + 0.86 * PET + 0.01 * P + 9.54 * LAI	20.9	0.70	17.5	0.68	653
Grassland (GR)	ET = −1.36 + 0.70 * PET + 0.04 * P + 6.56 * LAI	16.8	0.66	16.9	0.66	803
Deciduous broad leaf forest (DB)	ET = −14.82 + 0.98 * PET + 2.72 * LAI	23.7	0.74	17.8	0.73	754
Evergreen needle leaf forest (ENF)	ET = 0.10 + 0.64 * PET + 0.04 * P + 3.53 * LAI	17.8	0.68	17.1	0.68	1382
Evergreen broad leaf forest (EBF)	ET = 7.71 + 0.74 * PET + 1.85 * LAI	16.8	0.76	15.9	0.74	263
Mixed forest (MF)	ET = −8.763 + 0.95 * PET	13.1	0.79	12.6	0.79	259
Savannas (SVA)	ET = −25.66 + 0.18 * PET + 0.10 * P + 44.63 * LAI	11.1	0.68	34.2	0.00	36

RMSE, root of mean square error; ET, evapotranspiration; PET, potential evapotranspiration; P, precipitation; LAI, leaf area index.

Lumped ET models without separating land cover type

One of the main goals for this study was to test whether separating land cover type would improve model accuracy over 'lumped models' that were developed by pooling all data together. When pooling the entire datasets for all land cover types, the Type I models that consisted of three most significant variables had the following form:

$$\begin{aligned} \mathrm{ET} &= 0.16 + 0.51\,\mathrm{PET} + 0.1\,\mathrm{Rn} \\ R^2 &= 0.69, p < 0.0001,\ \mathrm{RMSE} = 21.4\ \mathrm{mm\ month^{-1}} \end{aligned} \quad (1)$$

The Type II model took the following form:

$$\begin{aligned} \mathrm{ET} &= -4.79 + 0.75\mathrm{PET} + 3.92\mathrm{LAI} + 0.04\mathrm{P} \\ R^2 &= 0.68, p < 0.0001,\ \mathrm{RMSE} = 18.1\ \mathrm{mm\ month^{-1}} \end{aligned} \quad (2)$$

The Type III model had the following form:

$$\begin{aligned} \mathrm{ET} &= -2.22 + 0.30{*}\mathrm{ET_o} + 6.32{*}\mathrm{LAI} + 0.09{*}\mathrm{P} \\ R^2 &= 0.49, p < 0.0001,\ \mathrm{RMSE} = 22.6\ \mathrm{mm\ month^{-1}} \end{aligned} \quad (3)$$

where PET is calculated by the Hamon's method, $\mathrm{ET_o}$ is the FAO crop reference ET, and VPD (hPa) is calculated from relative air humidity and air temperature.

Model collinearity analysis showed that the VIF values of independent variables varied from 1.2 to 4.4, indicating no co-linearity issues among the independent variables, and the three lumped models were robust.

Model evaluation

We evaluated the model strength in two broad ways. We examined whether ET models by ecosystem types provide overall improvement to predictions by generalized models (Type I, II, and III) by lumping all data (Equations (1)–(3). Comparisons of model performance in terms of R^2 and RMSE are presented in Tables IV, V, and VI. We also examined the accuracy of a land cover-specific ET model to predict ET at two conifer forest sites in California and Florida with contrasting climates and tree species.

Land cover-specific models versus a generalized model

When applying the generalized model (Type I, Equation 1) to each biomes, similar R^2 values for the majority of

Table VI. Type III models by land cover type developed using three FAO grass reference ET ($\mathrm{ET_o}$) and two commonly measured biophysical variables (precipitation and leaf area index).

Land cover type	Model by land cover (Type III)	Model by land cover type		Lumped model		
		RMSE	R^2	RMSE	R^2	n
Shrubland	ET = 0.14 * $\mathrm{ET_o}$ + 0.11 * P + 12.42 * LAI	12.1	0.73	14.8	0.53	213
Cropland (CRO)	ET = −8.6 + 0.44 * $\mathrm{ET_o}$ + 0.07 * P + 13.12 * LAI	20.5	0.68	16.9	0.67	584
Grassland (GR)	ET = 0.32 * $\mathrm{ET_o}$ + 0.075 * P + 10.28 * LAI	18.6	0.61	11.9	0.59	778
Deciduous broad leaf forest (DB)	ET = −12.4 + 0.50 * $\mathrm{ET_o}$ + 0.09 * P + 2.46 * LAI	20.9	0.64	16.2	0.61	874
Evergreen needle leaf forest (ENF)	ET = −4.0 + 0.34 * $\mathrm{ET_o}$ + 0.04 * P + 6.09 * LAI	15.2	0.70	12.8	0.68	1880
Evergreen broad leaf Forest (EBF)	ET = 12.7 + 0.44 * $\mathrm{ET_o}$ + 0.09 * P	23.3	0.49	14.4	0.42	197
Mixed forest (MF)	ET = −8.5 + 0.39 * $\mathrm{ET_o}$ + 0.04 * P + 4.22 * LAI	11.8	0.77	10.7	0.74	326
Savannas (SVA)	ET = −31.0 + 0.15 * $\mathrm{ET_o}$ + 0.05 * P + 47.67 * LAI	13.5	0.74	19.9	0.10	35

RMSE, root of mean square error; ET, evapotranspiration; PET, potential evapotranspiration; P, precipitation; LAI, leaf area index.

the biomes were found except for shrublands and savannas (Tables IV–6). For example, the lumped Type I model had much lower R^2 (0.39) and higher RMSE (25.9) than the land cover-specific model ($R^2 = 0.79$; RMSE = 14.0 mm) for shrublands (Table IV). Similarly, the lumped Type II models had much lower R^2 (0.64) and higher RMSE (18.8 mm) than land cover-specific model ($R^2 = 0.80$; RMSE = 12.5 mm) for shrubland (Table V). This was true for Shrubland for Type III model as well ($R^2 = 0.73$ for land cover-specific model vs $R^2 = 0.53$ for lumped model) (Table VI). For savannas, all three lumped models had very little predictive power ($R^2 < 0.1$; RMSE > 20 mm month^{-1}).

All data taken together, the land cover-specific models had slightly higher R (0.72) than the generalized simple model (Type II) as represented by Equation 2 ($R^2 = 0.68$) (Figure 7a and b). The land cover-specific models therefore explained slightly higher variance of ET than the generalized simple model. Similar results were found for other two models (not shown).

Model evaluations using two evergreen needleleaf forest (ENF) sites with a contrasting climate

To test whether the Type I models (Table IV) that used the three most influential variables might not always perform better than the simpler Type II models (Table V) or the

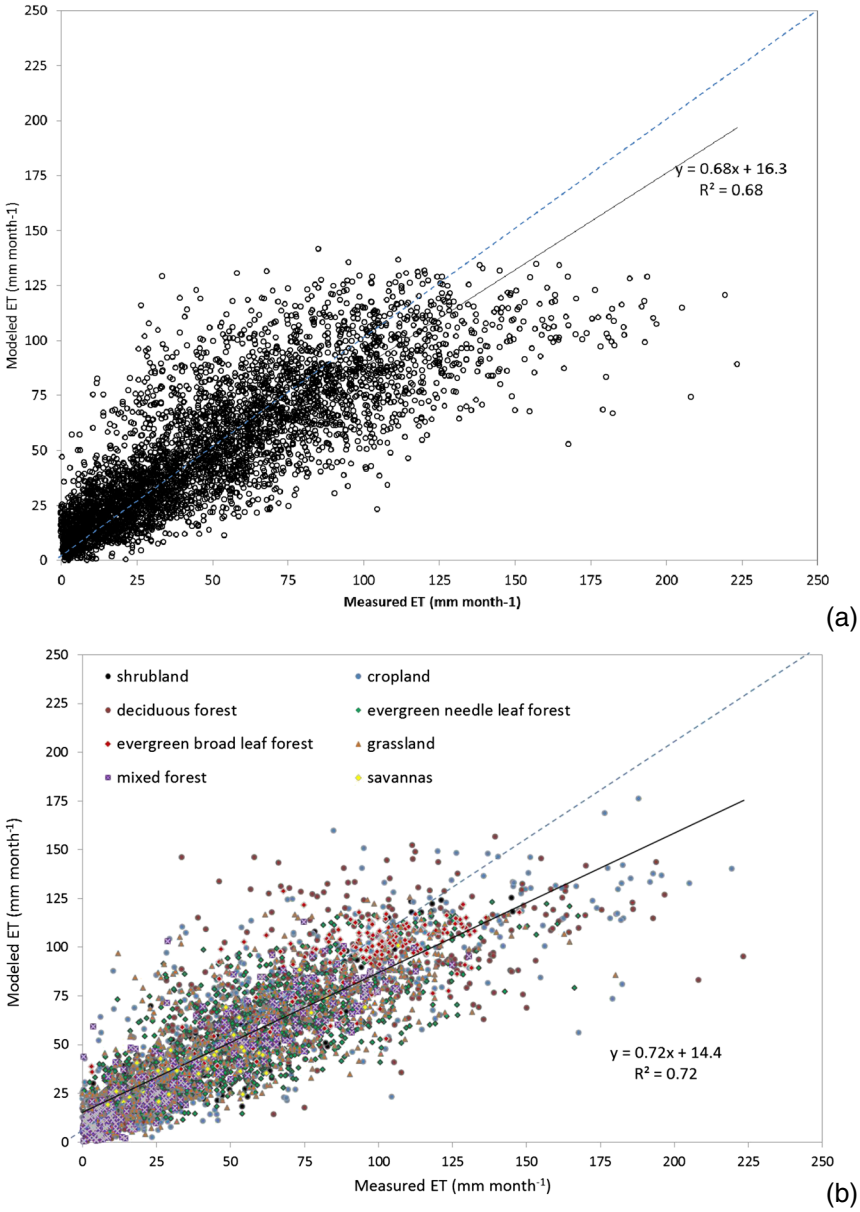

Figure 7. A comparison of measured and predicted ET using (a) a generalized Type II ET model and (b) models developed by land cover type.

most data-demanding Type III model, we evaluated two sets of ET models developed for evergreen needleleaf forest (ENF) at two eddy flux sites with contrasting climate and tree species: the Blodgett Forest (US-Blo) located in northern California (N38.89, W−120.63) (Goldstein *et al*., 2000; Thornton *et al*., 2002) with measurements from 2000 to 2006 and a young slash pine (*Pinus elliottii*) plantation forest site (US-SP2) (locally called Mize track) located in north-central Florida (N29.76, W82.24) (Bracho *et al*., 2012). The US-Blo was dominated by vigorously growing (LAI > 4.0) young ponderosa pine (*Pinus ponderosa*). The climate was characterized as having a warm and dry summer, but wet winter (Figure 8). Thus, ET did not positively correlate with P at this site ($R = -0.37$), but highly correlated to PET ($R = 0.93$) or ET_o ($R = 0.95$). In contrast, the other recently established evergreen forest site (US-SP2) located in the humid north-central Florida was dominated by 2-year old stands in 2000. However, LAI for this site increased dramatically from less than 1.0 in 2001 to about 6.0, reflecting rapid tree growth and stand establishment (Bracho *et al*., 2012). The site had a low P and ET in winter and high P and ET in the summer (Figure 10), and therefore, monthly ET was highly correlated with PET ($R = 0.78$) and ET_o ($R = 0.75$) and weakly with P ($R = 0.25$).

Overall, all models captured the monthly ET patterns well in spite of the large inter-annual variability of P at the US-Blo site (Figure 8). The Type I models performed better that both Type II and Type III models during the early growing season (April–June). Both Type II and Type III models underestimated ET during the growing seasons. The underestimation of ET by the Type II and III models was likely caused by the fact that actual measured ET from this site exceeded PET and ET_o rates that were computed from a temperature-based PET model or using biological parameters for grass land surface (Tables V and VI). In addition to air temperature, other parameters such as Rn and stomatal conductance are likely important in controlling ET at the US-Blo site (Table IV). All models substantially underestimated ET in the peak growing season (July–August) at this site for some years, particularly 2005 and 2006 (Figure 9). The process-based Biome-BGC model also failed to match the high ET rate at this site in a cross-site model comparison study (Thornton *et al*., 2002). The differences of ET estimate among the three models were the lowest in the fall season and winter, highest in the spring, and the peak growing season of April–July (Figure 9). The differences among the three models were generally consistent over the seven year period (2000–2006) with a large annual variability in precipitation (1019–1851 mm).

In contrast, all models captured the monthly ET patterns at the Florida US-SP2 site fairly well, particularly in the dormant season (November–April) (Figures 10 and 11). Overall, the simplest Type II model for ENF performed best ($R^2 = 0.51$, 9% underestimate). The Type II and Type III models performed equally well, and both underestimated ET rates during the growing seasons, however. The largest differences among the three types of models were found during the peak growing season

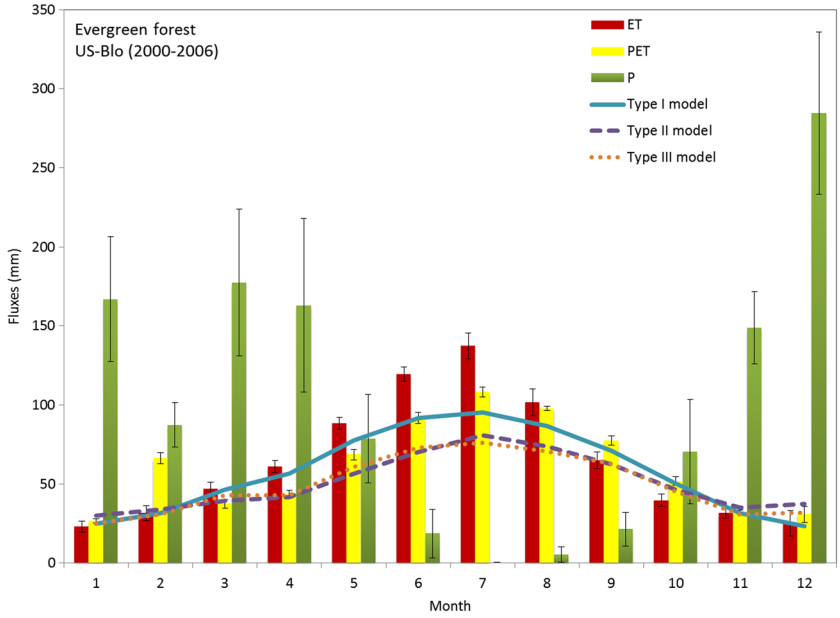

Figure 8. Mean monthly measured ET, P, and modelled PET and ET for a ponderosa pine plantation at Blodgett Forest for the period of 2000–2006 in California, western United States.

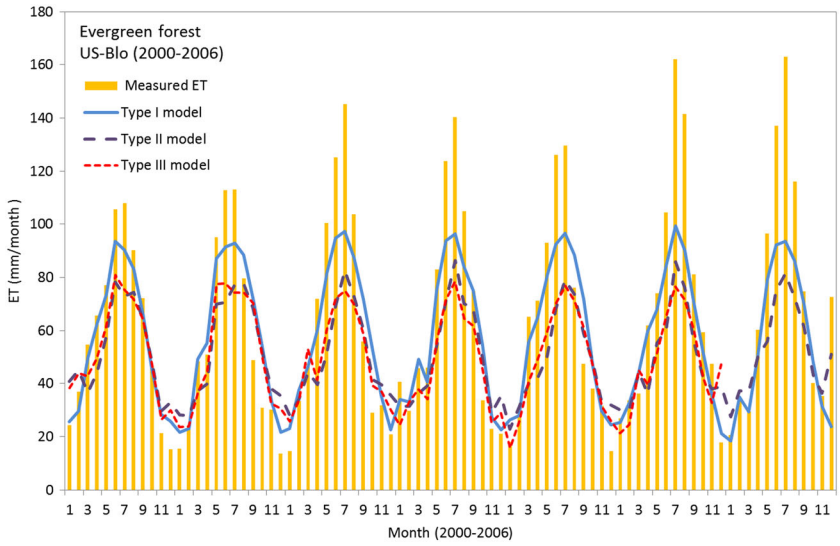

Figure 9. Monthly measured ET, P, and modelled PET and ET for a ponderosa pine plantation at Blodgett Forest for the period of 2000–2006 in California, western United States.

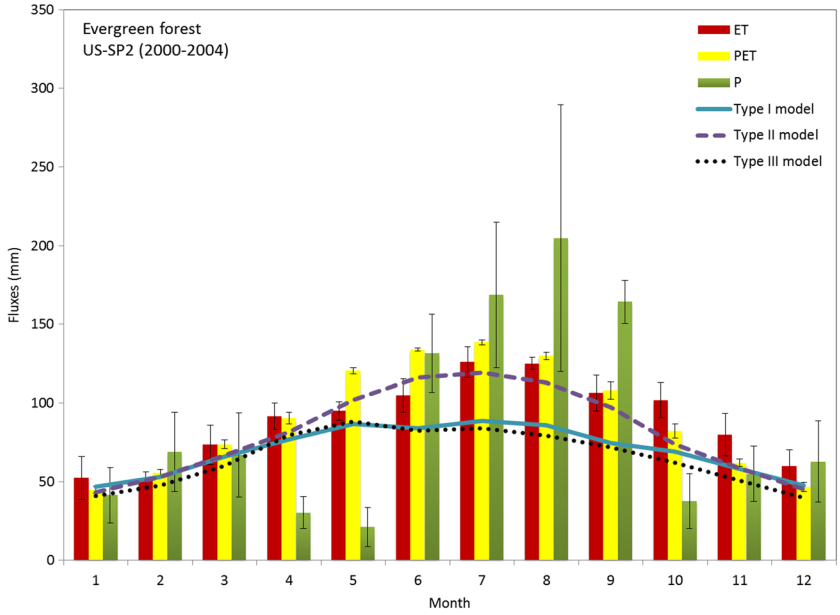

Figure 10. Mean monthly measured ET, P, and modelled PET and ET for slash pine plantation in north-central Florida for the period of 2000–2004 in the southeastern United States.

(Figures 10 and 11). ET closely followed PET ($R = 0.78$) (Figure 10) on this coastal plain landscape where groundwater was abundant and soil water stress was rare. The underestimation of ET by the Type I and Type II models suggested that the radiation-dominated ET model or reference ET model could not fully account for forest ET in a humid environment. A combination of LAI and PET might be best predictors for southern forest ET (Gholz and Clark, 2002; Sun *et al.*, 2010). Similar to the California site as discussed earlier, the differences of estimated ET were greatest during the growing season from May to September (Figures 10 and 11), suggesting that the biological controls to ET were not well captured in the Type I and III models. Although the Type II models provided good estimates for mean ET during the study period, they overestimated ET during the spring for the first three years but underestimated ET for almost all months during 2003–2004. The Type III models however performed best for the non-growing season. In the model evaluation, we used MODIS LAI for each site but did not use locally measured LAI to be consistent with model development and future applications.

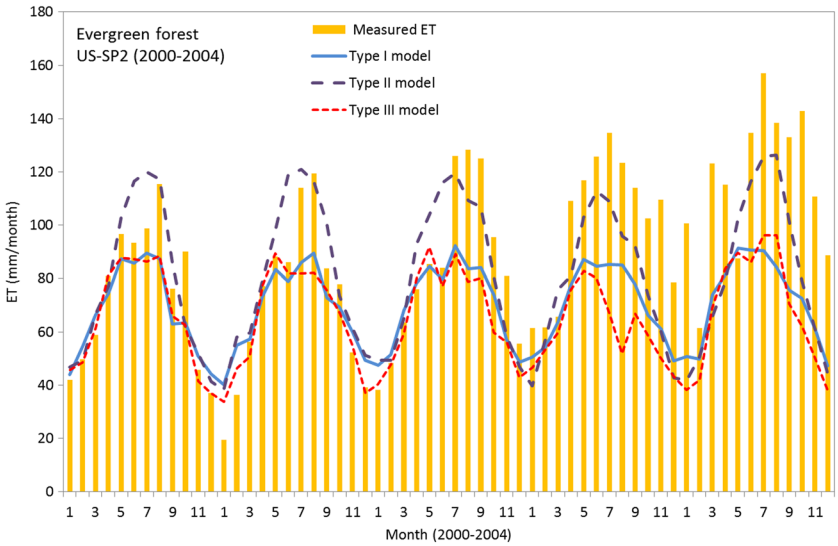

Figure 11. Monthly measured ET, P, and modelled PET and ET for slash pine plantation in north-central Florida for the period of 2000–2004 in the southeastern United States.

DISCUSSION

The FLUXNET network offers the best global ET data and opportunities to contrast monthly and annual scale water balance across multiple ecosystems (Baldocchi and Ryu, 2011). Our study showed that grasslands and shrublands were not necessarily found in areas with low precipitations, and ecosystem characteristics varied within each land cover type. The combinations of precipitation and ET determined water availability that eventually influenced ecosystem structure (e.g. biomass) functions (e.g. water yield). Our study reinforced the notion (Sun *et al.*, 2011a, b) that ecosystem water use (ET) and site hydrology were controlled by ecosystem characteristics and local climate (i.e. LAI, Ta or PET, Rn). These key factors explained the majority (60–90%) of the ET variability at the monthly scale.

Although the number of eddy covariance flux sites has dramatically increased exponentially in the past decade, the sample size of the FLUXNET used in this study for model development might still be limited and biased towards more mature ecosystems with little disturbance; therefore, a generalized model even for one land cover type may be biased. In addition, a generalized model may work well on average but can be biased during extreme conditions. Despite the potential biases, ecosystem level ET can be estimated with reasonable accuracy ($R^2 > 0.60$) using the models developed in this study with common environmental variables.

Environmental controls on monthly ET

It is well known that long-term mean ET for a region is controlled by precipitation and PET as described by the Budyko (1974) framework (Figure 5b) (Zhang *et al.*, 2001, 2004). The effects of vegetation characteristics (e.g. rooting depth) had significant effects on annual ET at the site to small watershed scale (Zhang *et al.*, 2001; Williams *et al.*, 2012) but relatively minor effects over large areas (Oudin *et al.*, 2008; Peel *et al.*, 2010; Sanford and Selnick, 2012). Our results generally support these claims at the monthly temporal scale. However, our study clearly showed that human disturbances such as irrigation altered the general long-term relationships among ET, PET, and P as presented in Budyko (1974) (Figure 5b).

Evapotranspiration analysis at the monthly scale offered new insights about broad biophysical controls on seasonal ET for the world's major ecosystem types. Overall, P or soil moisture content explained very small portion of the variance in ecosystem ET at the monthly scale, particularly for forests with high LAI and deeper roots with access to deep soil water storage. The insensitivity of ET to P indicated that these forests were rarely under water stress at the monthly scale. This finding was consistent with reports that mature forest ET was less variable than that of environmental conditions (Stoy *et al.*, 2006). Shrubland and grassland ecosystems showed higher responses to soil water stress, which was consistent with the findings of Stoy *et al.* (2006). The influence of P was not as large as that of LAI or Rn, suggesting that the variability of ET was mainly controlled by canopy structure (LAI) and energy (Rn) availability. A study by Nagler *et al.* (2007) found that for sparsely vegetated grassland and shrubland, ET was strongly correlated to leaf biomass (Enhanced Vegetation Index), moderately related to P, and weakly linked to Rn and Ta. The 'crop coefficient', ET/PET, can be readily predicted by LAI (Sumner and Jacobs, 2005). Our study is consistent with Nagler *et al.* (2007) in that LAI was the best predictor of ET for shrubland sites. An added benefit

of using LAI as an independent variable is that LAI can be used to scale-up ground ET measurements to the landscape scale in arid regions. The importance of Rn in affecting ET perhaps reflects the diversity of the shrub or grass sites across large climatic gradients. At the site level, LAI represents an overall integration of vegetation resource availability (i.e. soil water, absorbed light, and nutrition status) and ecosystem productivity, and thus is likely to dominate the control on ET (Chen *et al*., 2002; Nagler *et al*., 2007), particularly for deciduous forest (Xie *et al*., 2013), natural grasslands (Yang *et al*., 2007; Zhou *et al*., 2010; Yang and Zhou, 2011; Zheng *et al*., 2011), and herbaceous wetlands such as reed marsh (Zhou *et al*., 2010) that have dynamic phenology. Ecosystem structure information including LAI is more useful in explaining ET and water balance differences than land cover type.

Modelling ET under extreme drought conditions

Like any empirical model, our regression models were developed for normal climatic conditions and represented the mean ET controls across each ecosystem type. Thus, when applying the model to a particular site with unique vegetation structure (e.g. forest stand age not represented in the flux network site) or to a site for a particular time period (e.g. extreme droughts), the model may result in errors. For example, under specific circumstances such as certain dry regions where unique vegetation and climate are present, soil water stored in the top 10 cm of soil is the only water source to meet the demand of plants for long periods without precipitation (Kurc and Small, 2004). Thus, soil water storage coupled with other climatic variables controls ET of the current month, not necessarily the precipitation of the current month (Seneviratne *et al*., 2010). In such cases, underestimation errors may occur when using our modelling approach without considering soil moisture under extremely dry conditions. Nagler *et al*. (2007) considered inter-annual lags of precipitation to account for effects of soil water storage on ET. During model development in this study, we also tried to use total precipitation of previous month to account for precipitation lag time on ET. However, improvements by this approach were not always achievable for all sites. Soil moisture was measured only at the top 15 cm in majority of the FLUXNET sites and was found not a good factor in our initial analysis, and thus, later, we dropped this variable. In addition, our integrated hydrological modelling suggests that fully accounting soil moisture stress is essential to accurately model watershed scale ET and streamflow (Caldwell *et al*., 2012).

Model evaluation and limitation of the ET models and flux data. This study advances the lumped ET modelling approach previously presented by Sun *et al*. (2011a, 2011b) that used only 13 sites with limited ecosystem types represented. Here, we confirm that ecosystem-specific models are preferred in regional ecosystem flux upscaling and predictions (Xiao *et al*., 2012, 2014), especially for shrub lands and savannas. However, differences in species composition, plant stomatal conductance, phenology, age, and soil properties within the same ecosystem type may still contribute to modelling errors. Future studies should consider ecosystem properties such as canopy conductance and plant hydraulic conductivity at the species level. Other ET processes such as root hydraulic redistribution have not been included in a monthly scale model, but their cumulative effects can be significant (Domec *et al*., 2012b).

There are a few known sources of errors in measuring LE (i.e. ET) by the eddy covariance method (Leuning *et al*., 2012), including issues related to equipment that measures surface temperature (Kalma and Jupp, 1990) and wind speed (e.g. ultrasonic anemometers) (Nakai and Shimoyama, 2012). Along with the inevitable measurement errors, unknown disturbance, and instrument failure, deficiency of gap-filling techniques all contribute to the uncertainty of LE and thus accumulated monthly ET values. However, it is unclear if the systematic errors associated with eddy covariance instruments are also important for ET estimates at the ecosystem/landscape scale. A comprehensive review by Foken (2008) concluded that the eddy covariance method itself is designed for measuring energy fluxes for small, homogenous areas, and ET estimates are generally underestimated in most cases. Thus, Foken argued that the energy imbalance issues are scale problems and not necessarily instrument errors (also see Shao *et al*., 2014). In our study, the energy closure was $88 \pm 1\%$ for 6725 site-months records and was consistent with the findings of Wilson *et al*. (2002). The incomplete energy balance closure at FLUXNET sites caused underestimation of H and LE at a mean value of 12% in our study. The correction methods applied in this study to remedy energy closure errors could not guarantee that the ET estimates were correct because the method assumed approximately constant H/LE ratios.

As an essential input to our models, LAI derived from MODIS has significant uncertainty. Quite often, ground-based measurements of forest LAI are lower than LAI derived from MODIS especially for multi-layer forest stands. The monthly LAI is unrealistic in some cases. For example, at the Blodgett Forest site in California, LAI fell abruptly by 1.0 ($m^2\,m^{-2}$) in September 2001 but elevated back to a higher value in the following month. This abnormal phenomenon should not have occurred in an evergreen forest. Previous research by Cohen *et al*. (2006) also found that daily MODIS LAI fluctuated unrealistically. The misclassification of vegetation types also increased the errors of estimation when computing LAI by different

biomes (Pandya *et al*., 2006). In addition, the MODIS LAI had 1 km^2 resolution that was greater than the size of the fetch of eddy flux measurements for some sites. For example, the grassland site of US-DK1 was located at the Duke Forest open field adjacent to a mature forest. LAI for this site was registered as high as 5.5 in the summer and was apparently an over-estimate when comparing with similar grasslands that had an average LAI of less than 1.0. In addition, LAI values at the high end of the spectrum become more problematic because of 'saturation' of greenness. Reported MODIS LAI values for young stands were often found to be much higher that measured in the field. For example, the reported LAI for the US-SP2 site in 2000 was greater than 3.5, but the field measured value was less than 1.0 (Bracho *et al*., 2012). Such estimation errors in LAI could introduce uncertainty to model development and applications. Future studies should combine other remote sensing techniques, such as high resolution Landsat imagery to characterize LAI dynamics with a higher spatial resolution. Bridging the gaps between large spatial and temporal coverage (e.g. MODIS data) and flux footprint with spatial and spectral information from multiple sensors (e.g. Landsat) will improve the estimation of ET for a large area (Gray and Song, 2012).

Our previous work (Sun *et al*., 2011a, b) and the current study show that PET, LAI, Rn, VPD, and water availability (SWC, P) in some cases are key variables for developing general predictive models at the monthly scale. However, because Rn and VPD were not readily available for regional applications, this study provided another set of ET models, referred as Type II, so that ET can be estimated at a regional scale despite the lack of Rn and VPD data. Our study actually indicated that adding more climate variables may not improve ET predictions when all ecosystems are considered (see Equations 1–3).

CONCLUSIONS

This multi-ecosystem study provided general relationships among terrestrial water loss, energy, water availability, and vegetation dynamics at a fine temporal scale (i.e. monthly) – a scale that most regional scale hydrological models use for global change studies. We developed three types of empirical ET models that have the potential to estimate monthly ET at ecosystem-to-regional scales with reasonable accuracy under mean climate conditions. Ultimately, the accuracy of ET estimates by modelling depends on data availability of both climate and biophysical parameters of ecosystem structure. Embedding the ET models developed in this study in integrated hydrological model may help to constrain the accuracy of predicting ET and other hydrologic fluxes. Accurately estimating seasonal ET remains to be difficult when ecosystem structure information and ET processes for different land covers are not well characterized. Future studies should evaluate and improve the monthly ET models by comparing modelling results with other ET products, such as results from ecosystem models and upscaling approaches, remote sensing products, sapflow, and soil water balance based estimates in different regions with different climatic and physiographic conditions.

ACKNOWLEDGEMENTS

This study was supported by the USDA Forest Service Eastern Forest Environmental Threat Assessment Center and by the DOE–BER Terrestrial Ecosystem Sciences Program (11-DE-SC-0006700-ER65189). This work used eddy covariance data acquired by the FLUXNET community and in particular by the following networks: AmeriFlux [U.S. Department of Energy, Biological and Environmental Research, Terrestrial Carbon Program (DE-FG02-04ER63917 and DE-FG02-04ER63911)], AfriFlux, AsiaFlux, CarboAfrica, CarboEuropeIP, CarboItaly, CarboMont, ChinaFlux, Fluxnet-Canada (supported by CFCAS, NSERC, BIOCAP, Environment Canada, and NRCan), GreenGrass, KoFlux, LBA, NECC, OzFlux, TCOS-Siberia, and the United States China Carbon Consortium (USCCC). We acknowledge the financial support to the eddy covariance data harmonization provided by CarboEuropeIP, FAO-GTOS-TCO, iLEAPS, Max Planck Institute for Biogeochemistry, National Science Foundation, University of Tuscia, Université Laval and Environment Canada, and U.S. Department of Energy, and the database development and technical support from Berkeley Water Center, Lawrence Berkeley National Laboratory, Microsoft Research eScience, Oak Ridge National Laboratory, University of California, Berkeley, and University of Virginia. This work also used MODIS land subset (Oak Ridge National Laboratory Distributed Active Archive Center (ORNL DAAC). 2011. MODIS subsetted land products, Collection 5). We thank the anonymous reviewers for their constructive comments on the manuscript.

REFERENCES

Allen RG, Smith M, Perrier A, Pereira LS. 1994. An update for the definition of reference evapotranspiration. *ICID Bulletin* **43**: 1–34.

Asrar G, Fuchs M, Kanemasu ET, Hatfield JL. 1983. Estimating absorbed photosynthetic radiation and leaf area index from spectral reflectance in wheat. *Agronomy Journal* **76**(2): 300–306.

Baldocchi DD, Ryu Y. 2011. A synthesis of forest evaporation fluxes – from days to years – as measured with eddy covariance. In *Forest Hydrology and Biogeochemistry*, Levia DF, 599 Carlyle-Moses D, Tanaka T (eds). Springer: Heidelberg, Germany; 101–115.

Baldocchi DD, Falge E, Gu L, Olson R, Hollinger D, Running S, Anthoni P, Bernhofer C, Davis KJ, Evans R, Fuentes J, Goldstein A, Katul G, Law BE, Lee Z, Malhi Y, Meyers Z, Munger JW, Oechel W, Paw UKT,

Pilegaard K, Schmid HP, Valentini R, Verma S, Vesala T, Wilson KB, Wofsy S. 2001. FLUXNET: a new tool to study the temporal and spatial variability of ecosystem-scale carbon dioxide, water vapor, and energy flux densities. *Bulletin of the American Meteorological Society* **82**(11): 2415–2434.

Beer C, Reichstein M, Ciais P, Farquhar GD, Papale D. 2007. Mean annual GPP of Europe derived from its water balance. *Geophysical Research Letters* **34**, L05401, DOI:10.1029/2006GL029006.

Beer C, Reichstein M, Tomelleri E, Ciais P, Jung M, Carvalhais N, Rödenbeck C, Altaf Arain M, Baldocchi D, Bonan GB, Bondeau A, Cescatti A, Lasslop G, Lindroth A, Lomas M, Luyssaert S, Margolis H, Oleson KW, Roupsard O, Veenendaal E, Viovy N, Williams CA, Woodward I, Papale D. 2010. Terrestrial gross carbon dioxide uptake: global distribution and covariation with climate. *Science* **329**(5993): 834–838. DOI:10.1126/science.1184984.

Bonan GB. 2008. Forests and climate change: forcings, feedbacks, and the climate benefits of forests. *Science* **320**: 1444–1449.

Bosch JM, Hewlett JD. 1982. A review of catchment experiments to determine the effect of vegetation changes on water yield and evapotranspiration. *Journal of Hydrology* **55**(1–4): 3–23.

Bracho RG, Starr G, Gholz HL, Martin TA, Cropper WP, Loescher HW. 2012. Controls on carbon dynamics by ecosystem structure and climate for southeastern U.S. slash pine plantations. *Ecological Monographs* **82**: 101–128. DOI:10.1890/11-0587.1

Budyko MI. 1974. *Climate and Life*. Academic: New York.

Caldwell PV, Sun G, McNulty SG, Cohen EC, Moore Myers JA. 2012. Impacts of impervious cover, water withdrawals, and climate change on river flows in the conterminous US. *Hydrology Earth System Science* **16**: 2839–2857. DOI:10.5194/hess-16-2839-2012.

Chen J, Falk M, Euskirchen E, Paw UKT, Suchanek TH, Ustin SL, Bond BJ, Brosofske KD, Phillips N, Bi R. 2002. Biophysical controls of carbon flows in three successional Douglas-fir stands based on eddy-covariance measurements. *Tree Physiology* **22**: 169–177.

Chen J, Paw UKT, Ustin SL, Suchanek TH, Bond BJ, Brosofske KD, Falk M. 2004. Net ecosystem exchanges of carbon, water and energy in young and old growth Douglas-fir forests. *Ecosystems* **7**: 534–544.

Cheng L, Xu Z, Wang D, Cai X. 2011. Assessing interannual variability of evapotranspiration at the catchment scale using satellite-based evapotranspiration data sets. *Water Resources Research* **47**(9W09509): .

Cohen WB, Maiersperger TK, Turner DP, Ritts WD, Pflugmacher D, Kennedy RE, Kirschbaum A, Running SW, Costa M, Gower ST. 2006. MODIS land cover and LAI collection 4 product quality across nine sites in the western hemisphere. *Geoscience and Remote Sensing, IEEE Transactions on* **44**(7): 1843–1857.

Cramer W, Kicklighter DW, Bondeau A, Churkina G, Nemry B, Ruimy A, Schloss AL, Intercomparison ThE. P. OF. ThE. P. NpP. M, 1999. Comparing global models of terrestrial net primary productivity (NPP): overview and key results. *Global Change Biology* **5**(S1): 1–15.

Domec JC, Sun G, Noormets A, Gavazzi M, Treasure E, Cohen E, Swenson JJ, McNulty SG, King J. 2012a. Water flux components and their responses to drought in two intensively managed coastal plain loblolly pine forests: method comparisons. *Forest Science* **58**(5): 497–512.

Domec JC, Ogee J, Noormets A, Jouangy J, Gavazzi MJ, Treasure EA, Sun G, McNulty SG, King JS. 2012b. The impact of soil texture and future climatic conditions on root hydraulic redistribution and consequences for the carbon and water budgets of Southern US pine plantations. *Tree Physiology* . DOI:10.1093/treephys/tps018.

Dunn SM, Mackay R. 1995. Spatial variation in evapotranspiration and the influence of land use on catchment hydrology. *Journal of Hydrology* **171**(1–2): 49–73.

Feng XM, Sun G, Fu BJ, Su CH, Liu Y, Lamparski H. 2012. Regional effects of vegetation restoration on water yield across the Loess Plateau, China, *Hydrology and Earth System Sciences* **16**: 2617–2628, 2012.

Foken T. 2008. The energy balance closure problem: an overview. *Ecological Applications* **18**: 1351–1367.

Gholz HL, Clark KL. 2002. Energy exchange across a chronosequence of slash pine forests in Florida. *Agricultural and Forest Meteorology* **112**: 87–102.

Goldstein AH, Hultman NE, Fracheboud JM, Bauer MR, Panek JA, Xu M, Qi Y, Guenther AB, W Baugh W. 2000. Effects of climate variability on the carbon dioxide, water, and sensible heat fluxes above a ponderosa pine plantation in the Sierra Nevada (CA). *Agricultural and Forest Meteorology* **101**(2): 113–129.

Gray JM, Song C. 2012. Mapping leaf area index using spatial, spectral and temporal information from multiple sensors. *Remote Sensing of Environment* **119**: 173–183.

Hamon WR. 1963. Computation of direct runoff amounts from storm rainfall. *International Association of Scientific Hydrology. Publication* **63**: 52–62.

Hollinger DY, Richardson AD. 2005. Uncertainty in eddy covariance measurements and its application to physiological models. *Tree Physiology* **25**(7): 873–885.

Hoy C. 2012. A hydrologic characterization of three headwater mountain wetlands in eastern Kentucky, USA. M.S. Thesis. University of Kentucky, USA.

Jackson RB, Anderson LJ, Pockman WT. 2000. Measuring water availability and uptake in ecosystem studies. In *Methods in Ecosystem Science*, Sala OE, Jackson RB, Mooney HA, Howarth RW (eds). Springer: New York, NY.; 199–214.

Jasechko S, Sharp ZD, Gibson JJ, Jean Birks S, Yi Y, Fawcett PJ. 2013. Terrestrial water fluxes dominated by transpiration. *Nature* . DOI:10.1038/nature11983.

Jung M, Reichstein M, Ciais P, Seneviratne SI, Sheffield J, Goulden ML, Bonan G, Cescatti A, Chen J, de Jeu R, ADolman AJ, Eugster W, Gerten D, Gianelle D, Gobron N, Heinke J, Kimball J, Law BE, Montagnani L, Mu Q, Mueller B, Oleson K, Papale D, Richardson AD, Roupsard O, Running SW, Tomelleri E, Viovy N, Weber U, Williams C, Wood E, Zaehle S, Zhang K. 2010. Recent decline in the global land evapotranspiration trend due to limited moisture supply. *Nature* **467**(7318): 951–954.

Justice CO, Vermote E, Townshend JRG, de Fries R, Roy DP, Hall DK, Salomonson VV, Privette JL, Riggs G, Strahler A, Lucht W, Myneni RB, Knyazikhin Y, Running SW, Nemani RR, Zhengming W, Huete AR, van Leeuwen W, Wolfe RE, Giglio L, Muller J, Lewis P, Barnsley MJ. 1998. The Moderate Resolution Imaging Spectroradiometer (MODIS): land remote sensing for global change research. *IEEE Transactions on Geoscience and Remote Sensing* **36**(4): 1228–1249.

Kalma JD, Jupp DLB. 1990. Estimating evaporation from pasture using infrared thermometry: evaluation of a one-layer resistance model. *Agricultural and Forest Meteorology* **51**(3–4): 223–246.

King JS, Ceulemans R, Albaugh JM, Dillen SY, Fichot R, Fischer M, Leggett Z, Sucre E, Trnka M, Zenone T, Ceulemans R, Albaugh JM, Dillen SY, Domec J. 2013. The challenge of lignocellulosic bioenergy in a water-limited world. *BioScience* **63**(2): 102–117, DOI:10.1525/bio.2013.63.2.6, 2013.

Kurc SA, Small EE. 2004. Dynamics of evapotranspiration in semiarid grassland and shrubland ecosystems during the summer monsoon season, central New Mexico. *Water Resources Research* **40** (W09305): 15.

Kustas WP, Norman JM. 1996. Use of remote sensing for evapotranspiration monitoring over land surfaces. *Hydrological Sciences Journal* **41**(4): 495–516.

Law BE, Falge E, Gu L, Baldocchi DD, Bakwin P, Berbigier P, Davis K, Dolman AJ, Falk M, Fuentes JD, Goldstein A, Granier A, Grelle A, Hollinger D, Janssens IA, Jarvis P, Jensen NO, Katul G, Mahli Y, Matteucci G, Meyers T, Monson R, Munger W, Oechel W, Olson R, Pilegaard K, Paw UKT, Thorgeirsson H, Valentini R, Verma S, Vesala T, Wilson K, Wofsy S. 2002. Environmental controls over carbon dioxide and water vapor exchange of terrestrial vegetation. *Agricultural and Forest Meteorology* **113**: 97–120.

Leuning R, van Gorsela E, Massman WJ, Isaac PR. 2012. Reflections on the surface energy imbalance problem. *Agricultural and Forest Meteorology* **156**: 65–74.

Li X, Liang S, Yuan W, Yu G, Cheng X, Chen Y, Zhao T, Feng J, Ma Z, Ma M, Liu S, Chen J, Shao C, Li S, Zhang X, Zhang Z, Sun G, Chen S, Ohta T, Varlagin A, Miyata A, Takagi K, Saiqusa N, Kato T. 2012. Estimation of evapotranspiration over the terrestrial ecosystems in China. *Ecohydrology* . DOI:10.1002/eco.1341.

Liu W, Hong Y, Khan SI, Huang M, Vieux B, Caliskan S, Grout T. 2010. Actual evapotranspiration estimation for different land use and land cover in urban regions using Landsat 5 data. *Journal of Applied Remote Sensing* **4**: 041873–14.

Lu J, Sun G, McNulty SG, Amatya DM. 2003. Modeling actual evapotranspiration from forested watersheds across the southeastern United States. *JAWRA Journal of the American Water Resources Association* **39**(4): 886–896.

Lu J, Sun G, McNulty SG, Amatya DM. 2005. A comparison of six potential evapotranspiration methods for regional use in the southeastern United States. *Journal of American Water Resources Association* **41**: 621–633.

Mackay DS, Ewers BE, Cook BD, Davis KJ. 2007. Environmental drivers of evapotranspiration in a shrub wetland and an upland forest in northern Wisconsin. *Water Resources Research* **43**(3): W03442.

Mahrt L. 1998. Flux sampling errors for aircraft and towers. *Journal of Atmospheric and Oceanic Technology* **15**(2): 416–429.

Marquard D. 1970. Generalized inverses, ridge regression, biased linear estimation, and nonlinear estimation. *Technometrics* **12**: 591–612.

Mayocchi CL, Bristow KL. 1995. Soil surface heat flux: some general questions and comments on measurements. *Agricultural and Forest Meteorology* **75**(1–3): 43–50.

McMahon TA, Peel MC, Lowe LR, Srikanthan R, McVicar TR. 2012. Estimating actual, potential, reference crop and pan evaporation using standard meteorological data: a pragmatic synthesis. *Hydrology and Earth System Sciences Discussions* **9**: 11829–11910, DOI:10.5194/hessd-9-11829-2012, 2012.

Mu Q, Heinsch FA, Zhao M, Running SW. 2007. Development of a global evapotranspiration algorithm based on MODIS and global meteorology data. *Remote Sensing of Environment* **111**(4): 519–536.

Mu Q, Zhao M, Running SW. 2010. Improvements to a MODIS global terrestrial evapotranspiration algorithm. *Remote Sensing of Environment* **115**(8): 1781–1800.

Mu Q, Zhao M, Running SW. 2011. Brief introduction to MODIS evapotranspiration data set (MOD16).ftp://ftp.ntsg.umt.edu/.autofs/NTSG_Products/MOD16/MOD16_global_evapotranspiration_description.pdf

Nagler PL, Glenn EP, Kim H, Emmerich W, Scott RL, Huxman TE, Huete AR. 2007. Relationship between evapotranspiration and precipitation pulses in a semiarid rangeland estimated by moisture flux towers and MODIS vegetation indices. *Journal of Arid Environments* **70**(3): 443–462.

Nakai T, Shimoyama K. 2012. Ultrasonic anemometer angle of attack errors under turbulent conditions. *Agricultural and Forest Meteorology* **162–163**: 14–26.

Oudin L, Andréassian V, Lerat J, Michel C. 2008. Has land cover a significant impact on mean annual streamflow? An international assessment using 1508 catchments. *Journal of Hydrology* **357**: 303–316. DOI:10.1016/j.jhydrol.2008.05.021.

Pandya MR, Singh RP, Chaudhari KN, Bairagi GD, Sharma R, Dadhwal VK, Parihar JS. 2006. Leaf area index retrieval using IRS LISS-III sensor data and validation of the MODIS LAI product over central India. *IEEE Transactions on Geoscience and Remote Sensing* **44**(7): 1858–1865.

Peel MC, McMahon TA, Finlayson BL. 2010. Vegetation impact on mean annual evapotranspiration at a global catchment scale. *Water Resource Research* **46**, W09508, DOI:10.1029/2009WR008233.

Ray SS, Dadhwal VK. 2001. Estimation of crop evapotranspiration of irrigation command area using remote sensing and GIS. *Agricultural Water Management* **49**(3): 239–249.

Running SW. 1984. Microclimate control of forest productivity: analysis by computer simulation of annual photosynthesis/ transpiration balance in different environments. *Agricultural and Forest Meteorology* **32**(3–4): 267–288.

Running SW, Nemani RR, Peterson DL, Band LE, Potts DF, Pierce LL, Spanner MA. 1989. Mapping regional forest evapotranspiration and photosynthesis by coupling satellite data with ecosystem simulation. *Ecology* **70**(4): 1090–1101.

Sanford WE, Selnick DL. 2012. Estimation of Evapotranspiration across the conterminous United States using a regression with climate and land-cover data. *Journal of the American Water Resources Association* **1–14**: . DOI:10.1111/jawr.12010.

SAS Institute Inc. 2008. *SAS/STAT® 9.2 User's Guide*. SAS Institute Inc.: Cary, NC.

Schmid HP. 1997. Experimental design for flux measurements: matching scales of observations and fluxes. *Agricultural and Forest Meteorology* **87**(2–3): 179–200.

Seneviratne SI, Corti T, Davin EL, Hirschi M, Jaeger EB, Lehner I, Orlowsky B, Teuling AJ. 2010. Investigating soil moisture–climate interactions in a changing climate: a review. *Earth-Science Reviews* **99**(3–4): 125–161.

Shao C, Li L, Dong G, Chen J. 2014. Spatial variation of net radiation and its contribution to energy balance closure in grassland ecosystems. *Ecological Processes* **3**(1): 1–11.

Shuttleworth WJ. 2012. *Terrestrial Hydrometeorology*. Wiley-Blackwell: Oxford, UK.

Smith DM, Allen SJ. 1996. Measurement of sap flow in plant stems. *Journal of Experimental Botany* **47**(12): 1833–1844.

Song Y, Wang J, Yang K, Ma M, Li X, Zhang Z, Wang X. 2011. A revised surface resistance parameterisation for estimating latent heat flux from remotely sensed data. *International Journal of Applied Earth Observation and Geoinformation* **17**: 76–84.

Stoy P, Katul GG, Siqueira MBS, Juang JY, Novick KA, McCarthy HR, Oishi AC, Uebelherr JM, Kim H-S, Oren R. 2006. Separating the effects of climate and vegetation on evapotranspiration along a successional chronosequence in the southeastern US. *Global Change Biology* **12**: 2115–2135.

Sumner DM, Jacobs JM. 2005. Utility of Penman–Monteith, Priestley–Taylor, reference evapotranspiration, and pan evaporation methods to estimate pasture evapotranspiration. *Journal of Hydrology* **308**: 81–104.

Sun G, Noormets A, Chen J, McNulty SG. 2008. Evapotranspiration estimates from eddy covariance towers and hydrologic modeling in managed forests in Northern Wisconsin, USA. *Agricultural and Forest Meteorology* **148**(2): 257–26754.

Sun G, Noormets A, Gavazzi1 MJ, McNulty SG, Chen J, Domec J-C, King JS, Amatya DM, Skaggs RW. 2010. Energy and water balance of two contrasting loblolly pine plantations on the lower coastal plain of North Carolina, USA. *Forest Ecology and Management* **259**: 1299–1310.

Sun G, Caldwell P, Noormets A, McNulty SG, Cohen E, Moore Myers JA, Domec J-C, Treasure E, Mu Q, Xiao J, John R, Chen J. 2011a. Upscaling key ecosystem functions across the conterminous United States by a water-centric ecosystem model. *Journal Geophysical Research* **116**: G00J05.

Sun G, Alstad K, Chen J, Chen S, Ford CR, Lin G, Liu C, Lu N, McNulty SG, Miao H, Noormets A, Vose JM, Wilske B, Zeppel M, Zhang Y, Zhang Z. 2011b. A general predictive model for estimating monthly ecosystem evapotranspiration. *Ecohydrology* **4**(2): 245–255.

Thompson JR, Green AJ, Kingston DG. 2014. Potential evapotranspiration-related uncertainty in climate change impacts on river flow: an assessment for the Mekong River basin. *Journal of Hydrology* **510**: 259–279.

Thornton PE, Law BE, Gholz HL, Clark KL, Falge E, Ellsworth DS, Goldstein AH, Monson RK, Hollinger D, Falk M, Chen J, Sparks JP. 2002. Modeling and measuring the effects of disturbance history and climate on carbon and water budgets in evergreen needleleaf forests. *Agricultural and Forest Meteorology* **113**(1): 185–222.

Tian H, Lu C, Chen G, Xu X, Liu M, Ren W, Tao B, Sun G, Pan S, Liu J. 2011. Climate and land use controls over terrestrial water use efficiency in monsoon Asia. *Ecohydrology* **4**: 322–340.

Tian S, Youssef MA, Skaggs RW, Amatya DM, Chescheir GM. 2012. Modeling water, carbon, and nitrogen dynamics for two drained pine plantations under intensive management practices. *Forest Ecology and Management* **264**: 20–36.

Twine TE, Kustas WP, Norman JM, Cook DR, Houser PR, Meyers TP, Prueger JH, Starks PJ, Wesely ML. 2000. Correcting eddy-covariance flux underestimates over a grassland. *Agricultural and Forest Meteorology* **103**(3): 279–300.

Valentini R, Matteucci G, Dolman AJ, Schulze ED, Rebmann C, Moors EJ, Granier A, Gross P, Jensen NO, Pilegaard K, Lindroth A, Grelle A, Bernhofer C, Grunwald T, Aubinet M, Ceulemans R, Kowalski AS, Vesala T, Rannik U, Berbigier P, Loustau D, Gumundsson J, Thorgeirsson H, Ibrom A, Morgenstern K, Clement R, Moncrieff J, Montagnani L, Minerbi S, Jarvis PG. 2000. Respiration as the main determinant of carbon balance in European forests. *Nature* **404**(6780): 861–865.

Vörösmarty CA, Federer CA, Schloss AL. 1998. Potential evaporation functions compared on US watersheds: possible implications for global-scale water balance and terrestrial ecosystem modeling. *Journal of Hydrology* **207**(3–4): 147–169.

Williams CA, Reichstein M, Buchmann N, Baldocchi D, Beer C, Schwalm C, Wohlfahrt G, Hasler N, Bernhofer C, Foken T, Papale D, Schymanski S, Schaefer K. 2012. Climate and vegetation controls on the surface water balance: synthesis of evapotranspiration measured across a global network of flux towers. *Water Resources Research* **48**(6): W06523.

Wilson KB, Hanson PJ, Mulholland PJ, Baldocchi DD, Wullschleger SD. 2001. A comparison of methods for determining forest evapotranspiration and its components: sap-flow, soil water budget, eddy covariance and catchment water balance. *Agricultural and Forest Meteorology* **106**(2): 153–168.

Wilson K, Goldstein A, Falge E, Aubinet M, Baldocchi DD, Berbigier P, Bernhofer C, Ceulemans R, Dolman H, Field C, Grelle A, Ibrom A, Law BE, Kowalski A, Meyers T, Moncrieff J, Monson R, Oechel W, Tenhunen J, Valentini R, Verma S. 2002. Energy balance closure at FLUXNET sites. *Agricultural and Forest Meteorology* **113**(1–4): 223–243.

Xiao J, Chen J, Davis KJ, Reichstein M. 2012. Advances in upscaling of eddy covariance measurements of carbon and water fluxes. *Journal of Geophysical Research–Biogeosciences* **117**, G00J01, DOI:10.1029/2011JG001889.

Xiao J, Ollinger SV, Frolking S, Hurtt GC, Hollinger DY, Davis KJ, Pan Y, Zhang X, Deng F, Chen J, Baldocchi DD, Law BE, Altaf Arain M, Desai AR, Richardson AD, Sun G, Amiro B, Margolis H, Ru L, Scott RL, Blanken PD, Suyker AE. 2014. Data-driven diagnostics of terrestrial carbon dynamics over North America. *ScienceDirect*. DOI:10.1016/j.agrformet.2014.06.013.

Xie J, Sun G, Chu HS, Liu J, McNulty SG, Noormets A, John R, Ouyang Z, Zha T, Li H, Guan W, Chen J. 2013. Long-term variability in the water budget and its controls in an oak-dominated temperate forest. *Hydrological Processes* . DOI:10.1002/hyp.10079.

Yang F, Zhou G. 2011. Characteristics and modeling of evapotranspiration over a temperate desert steppe in Inner Mongolia, China. *Journal of Hydrology* **396**: 139–147.

Yang F, Ichii K, White MA, Hashimoto H, Michaelis AR, Votava P, Zhu AX, Huete A, Running SW, Nemani RR. 2007. Developing a continental-scale measure of gross primary production by combining MODIS and AmeriFlux data through Support Vector Machine approach. *Remote Sensing of Environment* **110**(1): 109–122.

Zeng Z, Piao S, Lin X, Yin G, Peng S, Ciais P, Myneni RB. 2012. Global evapotranspiration over the past three decades: estimation based on the water balance equation combined with empirical models. *Environmental Research Letters* **7**: 014026.

Zhang L, Dawes WR, Walker GR. 2001. Response of mean annual evapotranspiration to vegetation changes at catchment scale. *Water Resources Research* **37**(2): 701–708.

Zhang L, Hickel K, Dawes WR, Chiew FHS, Western AW, Briggs PR. 2004. A rational function approach for estimating mean annual evapotranspiration. *Water Resources Research* **40**, W02502, DOI:10.1029/2003WR002710.

Zheng Y, Xie Z, Roberts C, An P, Li X, Zhou G, Shimizu H, Drake S. 2011. Modelling seasonal evapotranspiration of arid lands in China. *Hydrology Research* **42**(1): 40–49.

Zhou L, Zhou G, Liu S, Sui X. 2010. Seasonal contribution and interannual variation of evapotranspiration over a reed marsh (*Phragmites australis*) in Northeast China from 3-year eddy covariance data. *Hydrological Processes* **24**(8): 1039–1047.

Zhou J, Zhang Z, Sun G, Fang X, Zha T, McNulty SG, Chen J, Jin Y, Noormets A. 2013. Climate controls on the seasonal and interannual patterns of carbon exchanges of a poplar plantation in northern China. *Forest Ecology and Management* **300**: 33–42.

